Aerospace Structures Information and Analysis Center

Cross Flow
Over Double Delta Wings

Report No. TR-94-23

February 1994

Approved for public release; distribution is unlimited

19990518 048

DTIC QUALITY INSPECTED 4

Operated for the Flight Dynamics Directorate by CSA Engineering, Inc.

REPORT DOCUMENTATION PAGE	*Form Approved* *OMB No. 0704-0188*

1. AGENCY USE ONLY *(Leave blank)*	2. REPORT DATE	3. REPORT TYPE AND DATES COVERED
	February 1994	Final Report 04/11/93-01/31/94

4. TITLE AND SUBTITLE

Cross Flow Over Double Delta Wings

5. FUNDING NUMBERS

F33615-90-C-3211

6. AUTHOR(S)

Horace Russell, Reginald G. Williams

7. PERFORMING ORGANIZATION NAME(S) AND ADDRESS(ES)

CSA Engineering, Inc.
2850 W. Bayshore Road
Palo Alto, CA 94303

8. PERFORMING ORGANIZATION REPORT NUMBER

ASIAC-TR-94-23

9. SPONSORING/MONITORING AGENCY NAME(S) AND ADDRESS(ES)

Flight Dynamics Directorate
Wright Laboratory
Air Force Materiel Command
Wright-Patterson AFB, OH 45433-7562

10. SPONSORING/MONITORING AGENCY REPORT NUMBER

11. SUPPLEMENTARY NOTES

12a. DISTRIBUTION/AVAILABILITY STATEMENT

Approved for public release; distribution is unlimited

12b. DISTRIBUTION CODE

13. ABSTRACT *(Maximum 200 words)*

This aerodynamic flow field investigation of a double delta wing is the third part of an overall fluid-structure interaction investigation. It was preceded by an investigation of a vortex breakdown on a simple delta wing and on the Onera M-6 wing.

Vortex flow at high angles of attack cause problems with stability and control as well as premature structural fatigue. An improved understanding of the vortex breakdown process could allow a more effective method of transferring the aerodynamic loads from a computational fluid dynamic model to a corresponding structural response model.

The results obtained are the final steps in the development of an aerodynamic model for use in determining the structural response of a double-delta wing.

14. SUBJECT TERMS	15. NUMBER OF PAGES
Delta Wings, Vortex Structure, Computerized Fluid Dynamics Vortex Breakdown, Structural Response	25
	16. PRICE CODE

17. SECURITY CLASSIFICATION OF REPORT	18. SECURITY CLASSIFICATION OF THIS PAGE	19. SECURITY CLASSIFICATION OF ABSTRACT	20. LIMITATION OF ABSTRACT
Unclassified	Unclassified	Unclassified	

NSN 7540-01-280-5500

Standard Form 298 (Rev. 2-89)
Prescribed by ANSI Std. Z39-18
298-102

FOREWORD

This report was prepared by the Aerospace Structures Information and Analysis Center (ASIAC), which is operated by CSA Engineering, Inc. under contract number F33615-90-C-3211 for the Flight Dynamics Directorate, Wright-Patterson Air Force Base, Ohio. The report presents the work performed under ASIAC Task No. 61. This effort was sponsored by the CFD Research Branch, Aeromechanics Division, Flight Dynamics Directorate, WPAFB, Ohio, with Dr. Don Kinsey as the technical monitor. The Principal Investigator was Dr. Horace Russell, Assistant Dean, University of Maryland.

Approved by:

Gordon R. Negaard

Gordon R. Negaard
ASIAC Manager

J. C. Parekh

Jatin C. Parekh
Program Manager

Table of Contents

List of Figures

Introduction

This aerodynamic flow field investigation of a double delta wing is the third part of an overall fluid-structure interaction investigation that was initiated in January 1990. It was preceded by investigations of a simple delta[1] wing and the Onera M-6 wing[2]. The delta wing was investigated as a first step toward characterization of vortex breakdown. The characterization was a crucial first step toward understanding the vortex flow and the breakdown process, not in terms of indicators, but in terms of fundamental mechanisms associated with breakdown. The Onera wing was selected because it was one of the first test cases for verification of the TEAM code and both extensive computational and experimental data are available.

The advantage of delta shaped wings are well documented. In addition to enabling aircraft to perform efficiently at supersonic cruise conditions, the delta shape provides high lift and enhanced maneuverability at low speeds and moderate angles of attack. It has been demonstrated experimentally and computationally that the lift and maneuverability enhancements are produced by the strong vortices which originate at the sharp leading edges. However, it is also well recognized this vortex flow at high angles of attack may also cause problems with stability and control as well as premature structural fatigue at high angle of attack. In particular, at high angles of attack the vortex increases in size and undergoes large scale turbulent dissipation. This breakdown in organized vortex structures can account for up to a 30% loss of lift which can induce moments about the center of gravity resulting in stability and control problems.

An improved understanding of the vortex breakdown process could allow a more effective method of transferring the aerodynamic loads from a computational fluid dynamic model to a corresponding structural response model. Also, additional insight concerning the structural response could be gained that would allow improved designed methods to mitigate against premature structural fatigue. Since the observance of vortex bursting by Peckham and Atkinson[3],

the prediction of vortex bursting have been an active research area. All theories currently predict vortex breakdown to occur within a given range of swirl angles and to be sensitive to the axial pressure gradients. However, the theory does not provide flow detail in the vortex breakdown region nor the breakdown location with sufficient accuracy to compare with experimental results.

Approach

The geometry chosen for this research is based on the dimensions of previous experimental and computational studies[4,5,6,7]. Figure 1 is a non-dimensionalized planform view of the cropped double delta wing used in this study. This configuration is highly representative of today's modern aircraft. The strake or leading edge extension (LEX) and the wing have 76 and 40 degree sweep, respectively. This geometry is well suited for the problem at hand because of the significant length of the LEX and the large vortex structure at high angles of attack. Because zero sideslip was implemented only half the model was required with symmetry assumed at the centerline. Sharp leading edges were used and based on experimental evidence[8], the path of the leading edge vortex is significantly influenced by the leading edge shape. The edge shape will be discussed later in this report. Tests were for angles of attack of 0, 10, 16, and 27.4 degrees for inviscid calculations. A database created from Figure 1 was used to develop a three dimensional grid. This grid was then used in a finite volume flow solver to calculate specific flow properties over the model.

Grid Generation

The grid generation utilized for this study was Gridgen Version 8. This is a menu driven three dimensional interactive multiple block grid generation software package[9] created by MDA Engineering. The interactive capability allowed easy refinement of the grid during the

grid generation process. The computation time required to generate the volume grid was 15 minutes, which was reasonable compared to binary conversions, file transfers, and long queuing time necessary on a Cray super computer. Figure 2 is the final C-H grid used for this study. A total of 631,980 grid points defined the entire flow field. Both the surface grid and the three dimensional volume grid were generated on a Silicon Graphics Iris 4D workstation. The majority of the grid required an algebraic solver based on transfinite interpolation, but near the solid boundaries, an elliptic solver was used to patch the discontinuities that existed between the solid boundaries and the fluid boundaries. The Thomas-Middlecoff elliptic solver with fixed boundaries proved beneficial in resolving major grid discontinuities. A total of seven blocks were created for the near and far flow field. The model's upper and lower surfaces each used 45 grid points in the stream wise direction and 21 in the spanwise direction. The leading edge surface was defined by 45x15 grid points. Grid clustering was used along the leading edge to help resolve the flow properties in calculating the shear layer that separates and eventually forms the leading edge vortex. The fluid boundary was extended twelve chord lengths in all directions. The mesh size for the far field boundary in the upstream direction was maintained as uniformed and as large as possible. The Gridgen code has a subroutine to check for grid skewness and negativity, neither of which existed in the grid. Once the initial grid was developed, computational runs were made. Based on these results, the grid was continually modified until solutions were obtained that compared favorably to experimental and computational data. This consumed a vast amount of research time because no standard gridding procedure exists for all configurations of interest.

Computational Algorithm

The computational algorithm used for the inviscid computation was the Three-dimensional Euler/Navier-Stokes Aerodynamic Method (TEAM)[10] code. This is a finite volume multistage time-stepping

algorithm. Convergence can be enhanced using enthalpy damping, second and fourth order viscous dissipation, and a choice of five numerical dissipation schemes. The TEAM code had been developed to work in all flight regimes from subsonic to hypersonic. Verification of leading edge vortical flow has been documented using the code[10].

For this study, inviscid computation was performed at a mach number of 0.25 and the previously stated angles of attack. Implicit residual smoothing in the i,j, and k directions enhanced the convergence time. Additionally, a standard adaptive viscous dissipation scheme that blended second and fourth order differences was evoked. The values chosen for the dissipation relied on the free stream mach number and the coarseness of the grid. The numerical dissipations were evaluated twice per time step and the default values for the four-stage time stepping scheme were 1/4, 1/3, 1/2, and 1. Convergence based on root-mean-squared averaging of the mass flux residual was obtained in 1000-2000 iterations.

Solutions

Figures 3 to 14 show results obtained for the double delta wing and these were compared to results obtained by Kern[4] and show excellent agreement for the flow visualization using trace particles, swirl magnitude, and pressure coefficient. These figures support the well established trends in the vortex patterns over double delta wings. At zero degrees the strake vortex is weak and the wing vortex is almost nonexistent. As the angle of attack is increased from 0 to 16 degrees the strake vortex increases in strength and after the strake-wing juncture moves outward over the wing surface. The two vortices become entwined between 0 and 10 degrees, and this phenomenon is more pronounced at 16 degrees. At these lower angles of 10 and 16 degrees the vortex will burst some distance downstream of the trailing edge. As the angle is still increased the vortex burst region moves upstream and will eventually exist over the delta wing (Figure 6 and 7). Figure 7 shows in greater detail trace particles emanating from all the

surface grid points at 27.4 degrees. Note how the vortex core maintains the same diameter upstream of the burst region. In Figure 7, the onset of vortex breakdown is approximately two-thirds the chord length from the strake apex. At this point, the vortex core rapidly expands causing a decrease in the axial velocity. This leads to an adverse pressure gradient resulting in reverse and separated flow. Although the vortex breakdown has already occurred at 27.4 degrees, there is a substantial amount of lift created by the otherwise highly-structured vortex upstream of breakdown. These overall trends have been well established in existing literature and were observed in the initial investigation involving a 70 degree sweep single delta wing[1]. Figures 8 and 9 reiterate the above discussion by showing the three dimensional aspects of the vortex development at 10 and 27.4 degrees. At 10 degrees, the region of vorticity is relatively close to the wing surface and limited in volume compared to the vortex field at 27.4 degrees.

A comparison between surface grid structures used by Kern and the one used in this study is shown in Figure 10. What is readily observable is that Kern used a larger amount of grid clustering along the leading edge because the focus of that study was to examine the effects of deployable surfaces in the strake-wing junction. This resulted in increased resolution of the vortex generated from this region. Kern's results are compared in Figures 11 and 12 for 10 and 16 degrees angle of attack. At 10 degrees, the strake and wing vortices have begun to merge over the wing surface, but Kern shows greater detail regarding the portion of the strake vortex that remains independent of the wing vortex. This is consistent with the difference in grid clustering. In Figure 12, at 16 degrees, the two results are very similar. The only noticeable difference is the occurrence of a few trace particles emanating from the strake-wing junction in Kern's results that are convected downstream with less movement away from the centerline. Again, this is probably the effects of denser grid clustering which is capable of resolving the large gradients that exist in the separating shear layer at the leading edge. Although the increased grid clustering shows better detail of the leading edge

vortex, the major trends in vortex migration and breakdown remain highly similar between the two studies.

Figures 13 and 14 show the swirl magnitude and pressure coefficient, respectively, for the flow field above the wing at two chord locations. Both figures show cross-sections of the flow at 55% (pre-burst) and 85% (post-burst) chord. In Figure 13 the magnitude of the swirl drops significantly downstream of the breakdown location. Likewise, the pressure coefficient increases after breakdown indicating a decrease in the local velocity. Additionally, the contour levels for the swirl and the pressure coefficient are more intense and structured upstream of the vortex burst region indicating a well defined vortex pattern.

The results obtained are the final steps in the development of an aerodynamic model for use in determining the structural response of the double-delta wing. Small enhancements to the grid to improve the code's performance will be made, including less grid points to reduce the computational time and increased grid clustering along the leading edge. Additionally, viscous solutions will be obtained with the TEAM code to better understand the role viscosity plays in the vortex breakdown phenomenon and in the development of secondary and tertiary vortices. Finally, the TEAM code results will be used as input to PATRAN to preprocess and post-process data for NASTRAN. NASTRAN will be used to calculate the dynamic loads and deflections caused by vortex breakdown and vortices impinging on the lifting surfaces.

Acknowledgements

The authors would like to thank Dr. Don Kinsey of the Applied CFD Group of the Flight Dynamics Lab at Wright-Patterson AFB for supporting this research. Special thanks also goes to Howard Emsley, John Seo, Greg Sharp, Bill Strang, and Frank Witzeman at Wright-Patterson for their technical support and recommendations.

Additionally, the continuing support from the Pittsburgh Supercomputing Center is very much appreciated.

Bibliography

1. Craig, S., Characterization of Vortex Breakdown Over a 70 Degree Delta Wing, M.S. Scholarly Paper, University of Maryland Department of Mechanical Engineering, 1993.

2. King, K., Fluid-Structure Interaction Methodology, M.S. Thesis, University of Maryland Department of Mechanical Engineering, 1992.

3. Peckham, D.H. and Atkinson, S.A., "Preliminary Results of Low Speed Wind Tunnel Tests on a Gothic Wing of Aspect Ratio 1.0', ARC CP508.

4. Kern, S.B., "Numerical Investigation of Vortex Flow Control Through Small Geometry Modifications at the Strake/Wing Junction of a Cropped Double-Delta Wing", AIAA Paper 92-0411, 30th Aerospace Sciences Meeting and Exhibit, January 6-9, 1992.

5. Coutley, R. L., Numerical Studies of Compressible Flow Over a Double-Delta Wing at High Angles of Attack, M.S. Thesis Naval Postgraduate School, Monterey, California, March 1990.

6. den Boer, R.G. and Cunningham, A.M., "Low Speed Unsteady Aerodynamics of a Pitching Straked Wing at High Incidence-Part I: Test Program", Journal of Aircraft, Vol. 27, No. 1, January 1990, pp. 23-30.

7. den Boer, R.G. and Cunningham, A.M., "Low Speed Unsteady Aerodynamics of a Pitching Straked Wing at High Incidence-Part II: Harmonic Analysis", Journal of Aircraft, Vol. 27, No. 1, January 1990, pp .31-41.

8. Kegelman, J.T. and Roos, F.W., "Effects of Leading-Edge Shape and Vortex Burst on the Flowfield of a 70-Degree-Sweep Delta Wing", AIAA Paper No. 89-0086.

9. The Gridgen Version 8 Multiblock Grid Generation User's Manual, 1992, MDA Engineering, Inc. Arlington, Texas.

10. Three-dimensional Euler/Navier-Stokes Aerodynamic Method (TEAM) User's Manual, Volume I,II, and III. AFWAL-TR-87-3074.

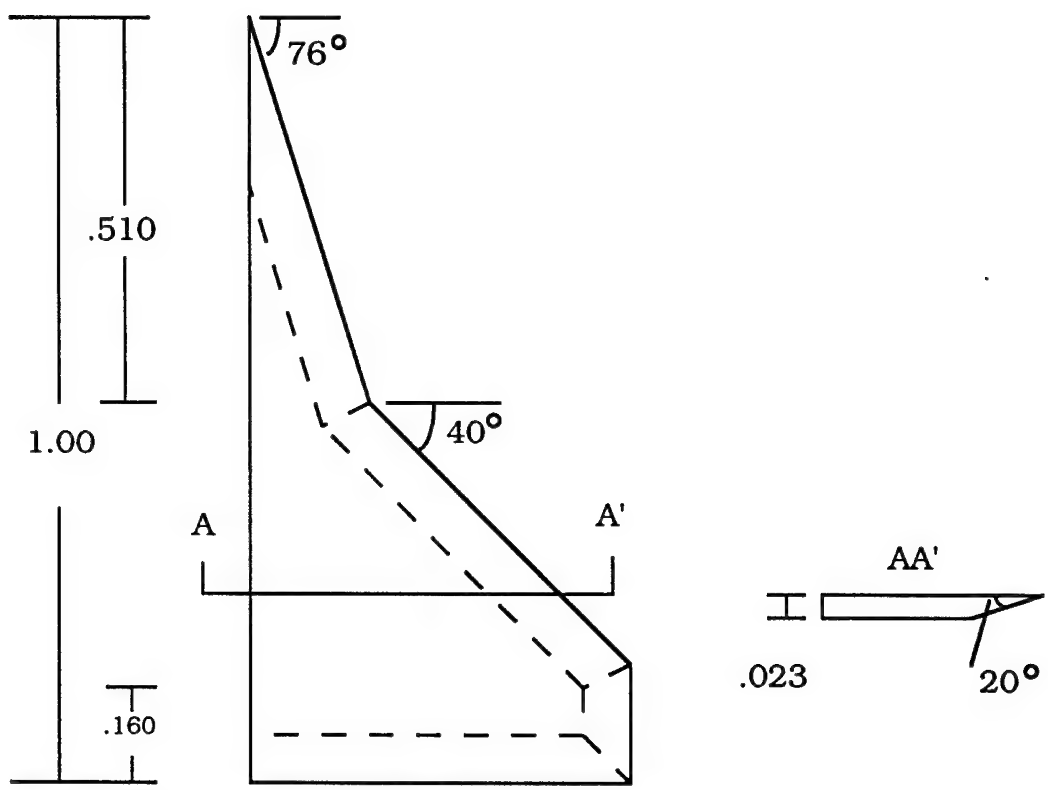

Figure 1. Double delta wing configuration.

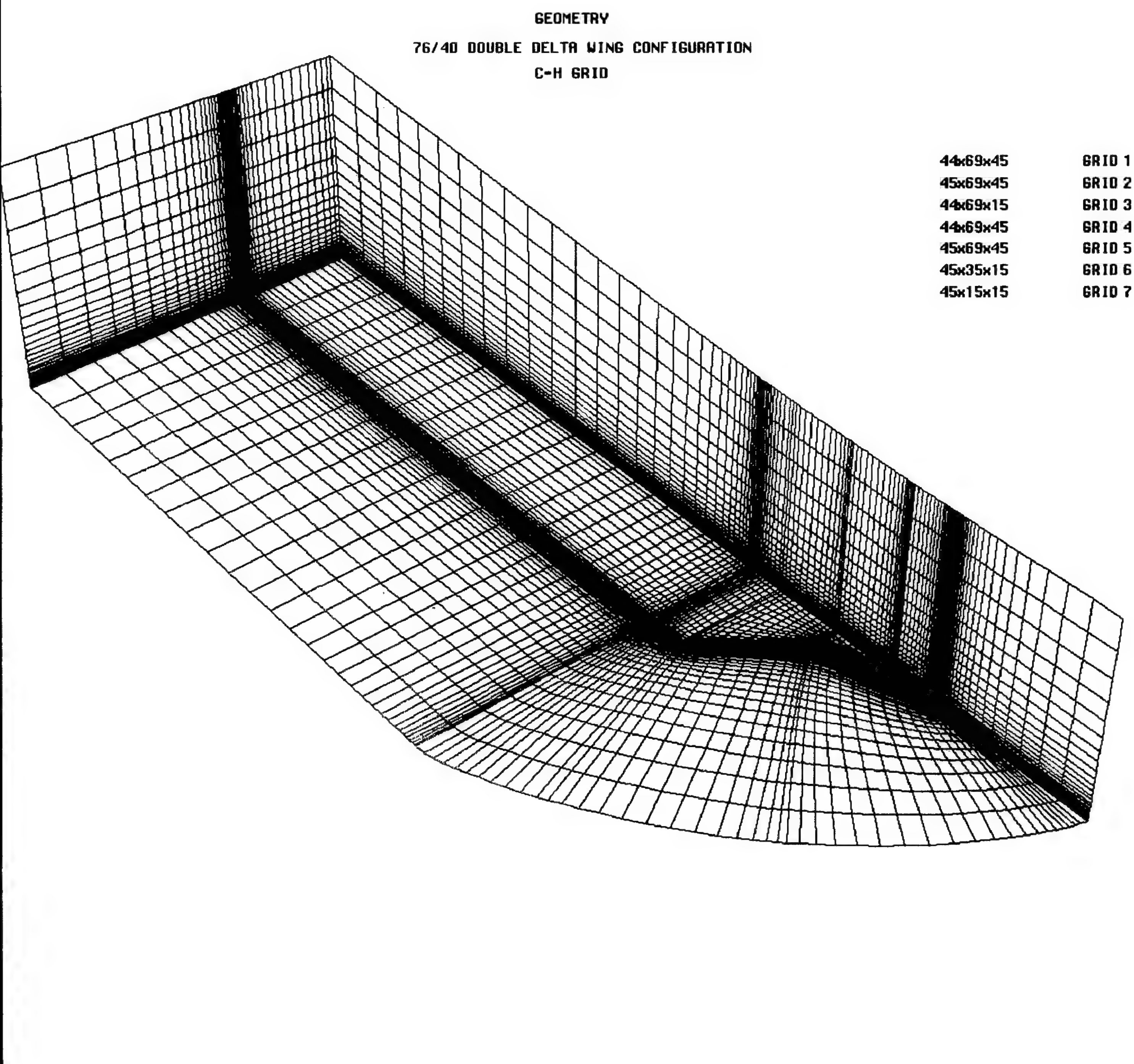

Figure 2. C-H grid topography.

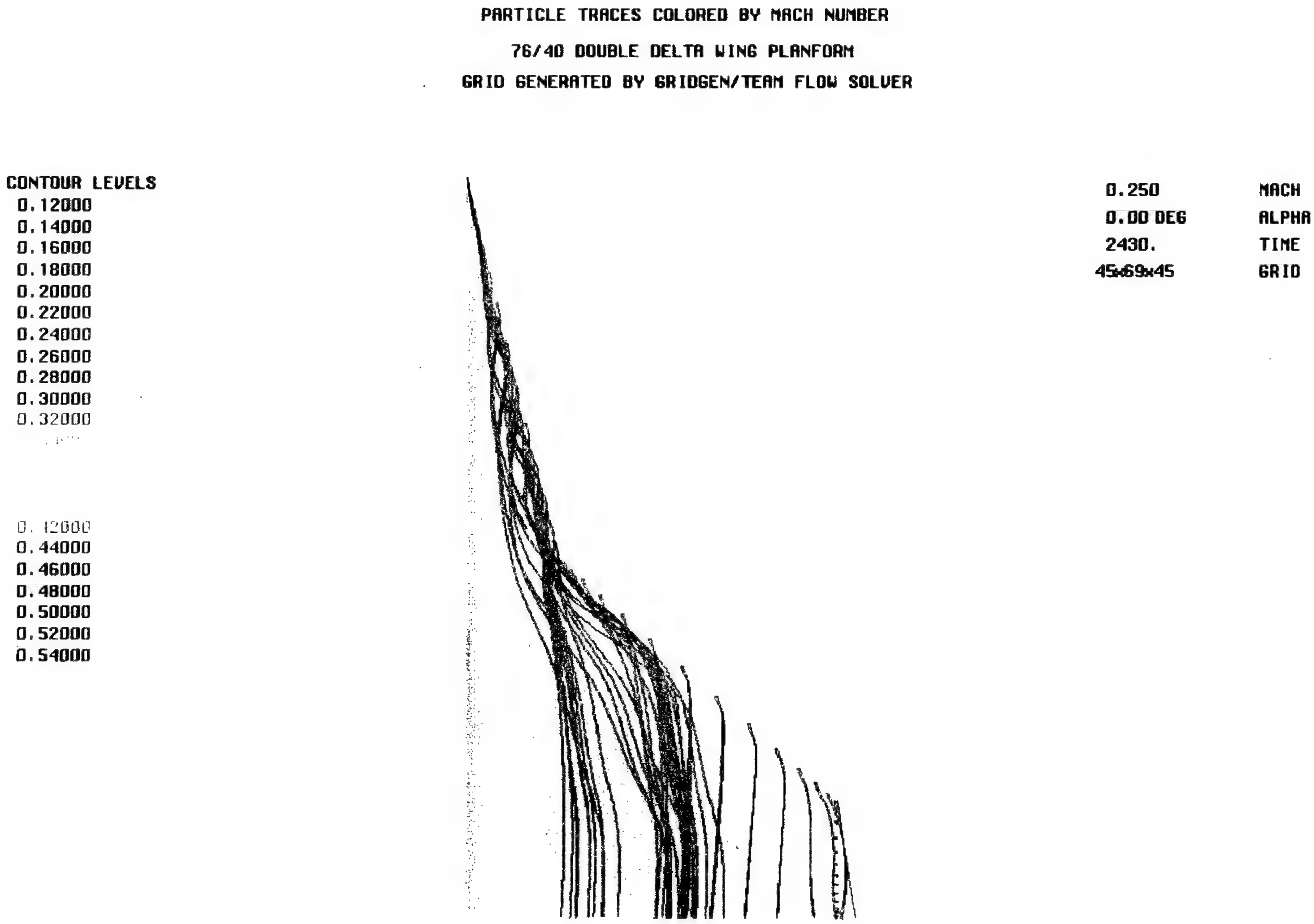

Figure 3. Particle trace colored by mach number, α=0.0 degrees.

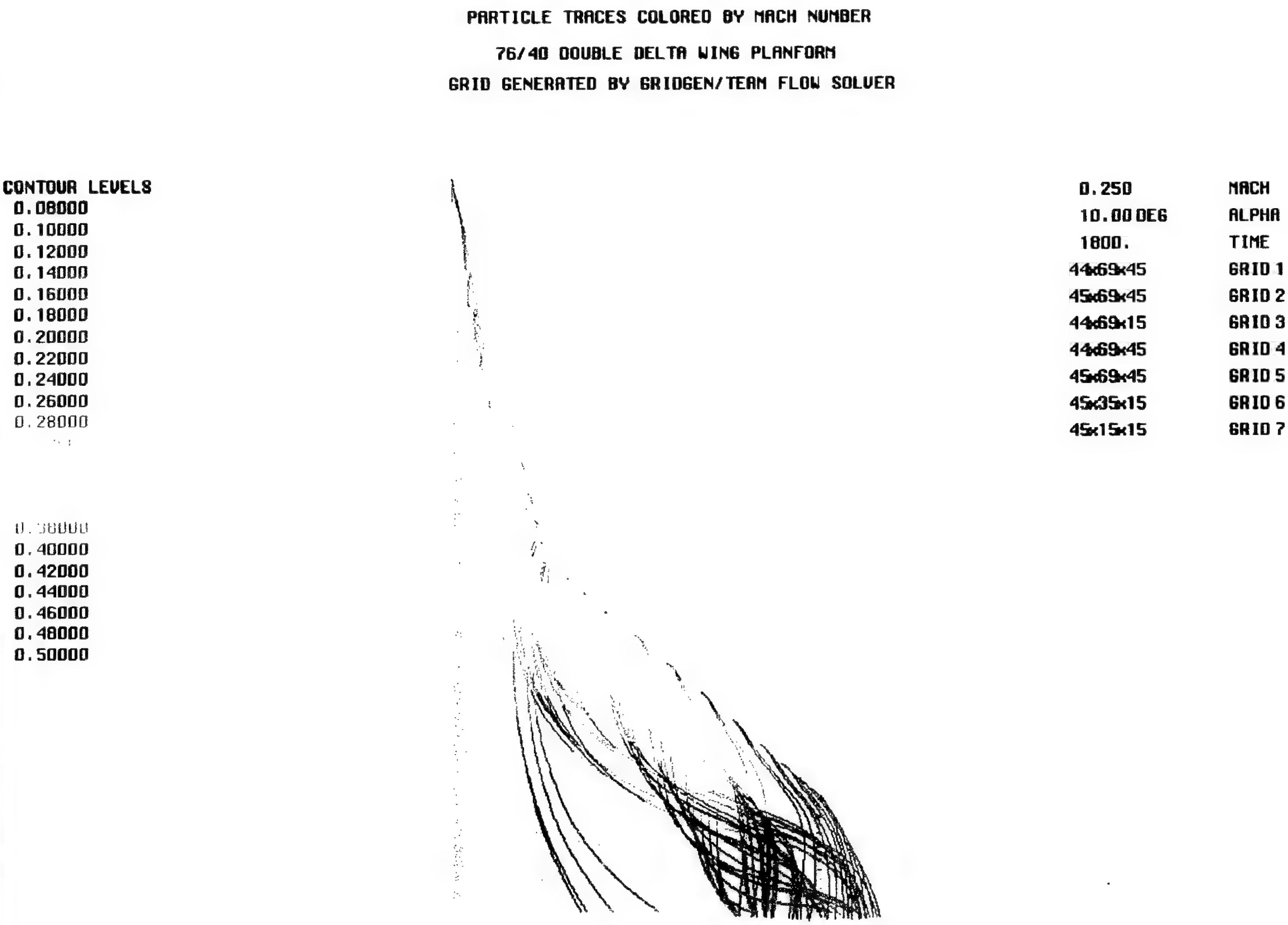

Figure 4. Particle trace colored by mach number, α=10.0 degrees.

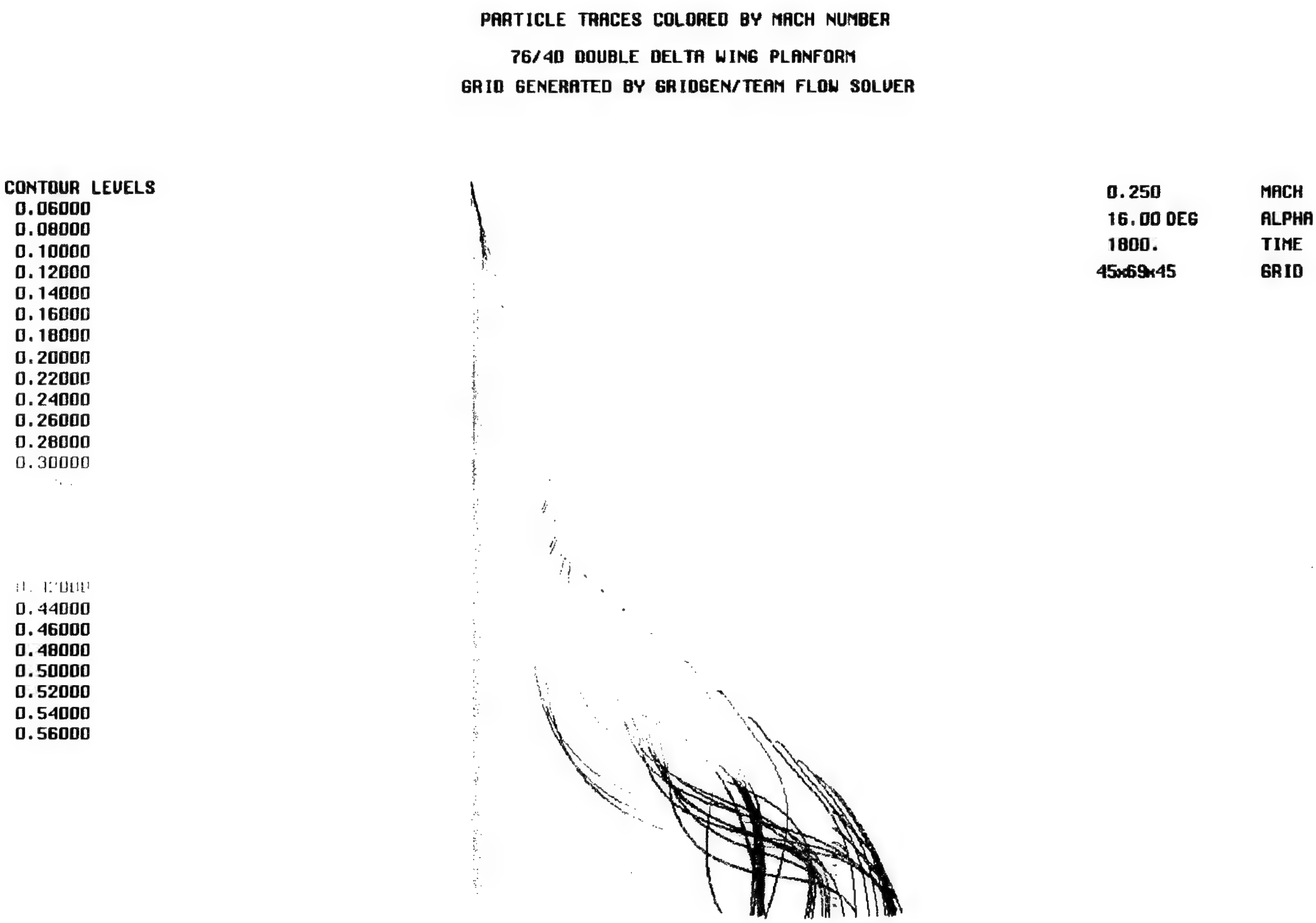

Figure 5. Particle trace colored by mach number, α=16.0 degrees.

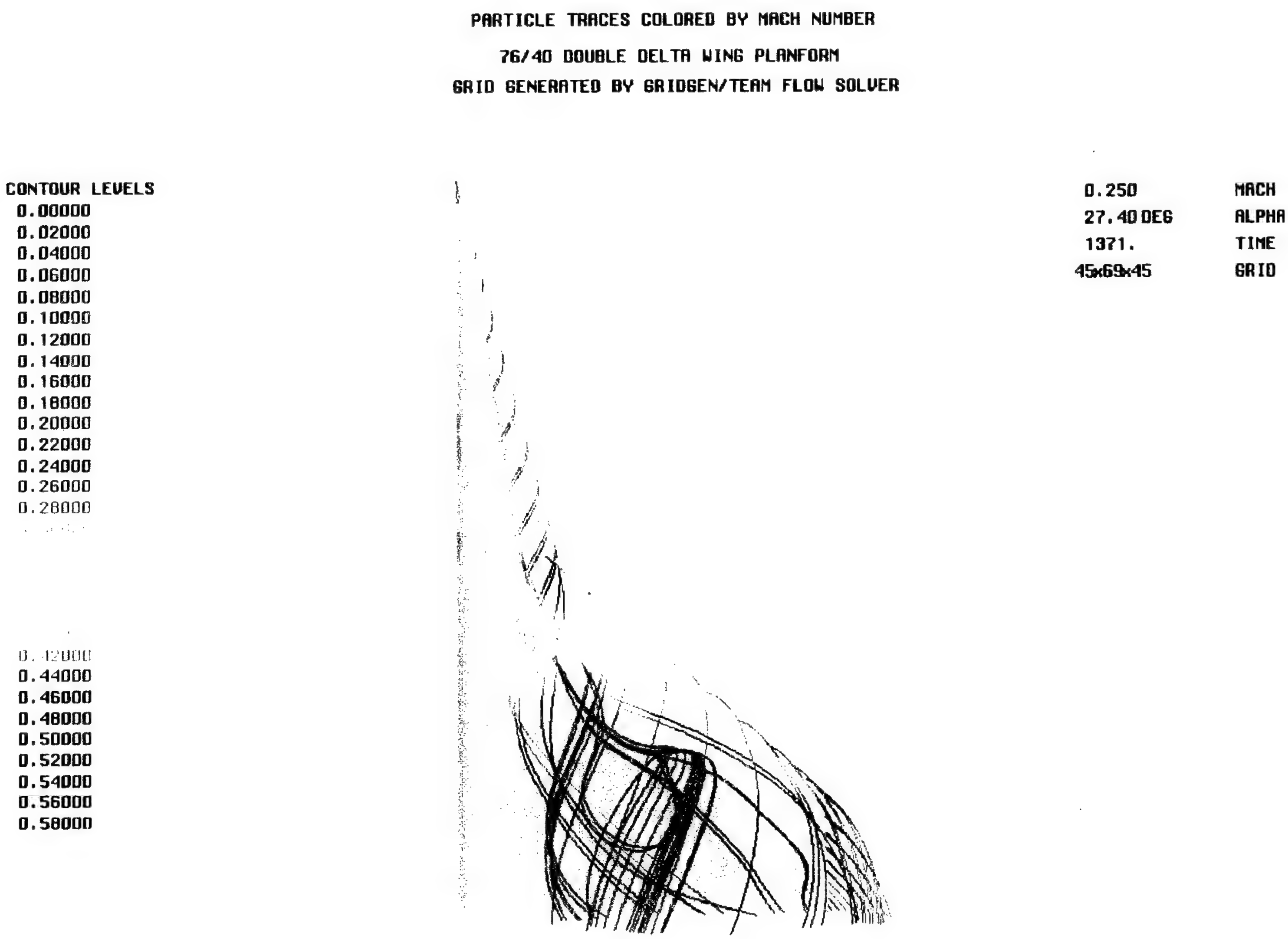

Figure 6. Particle trace colored by mach number, α=27.4 degrees.

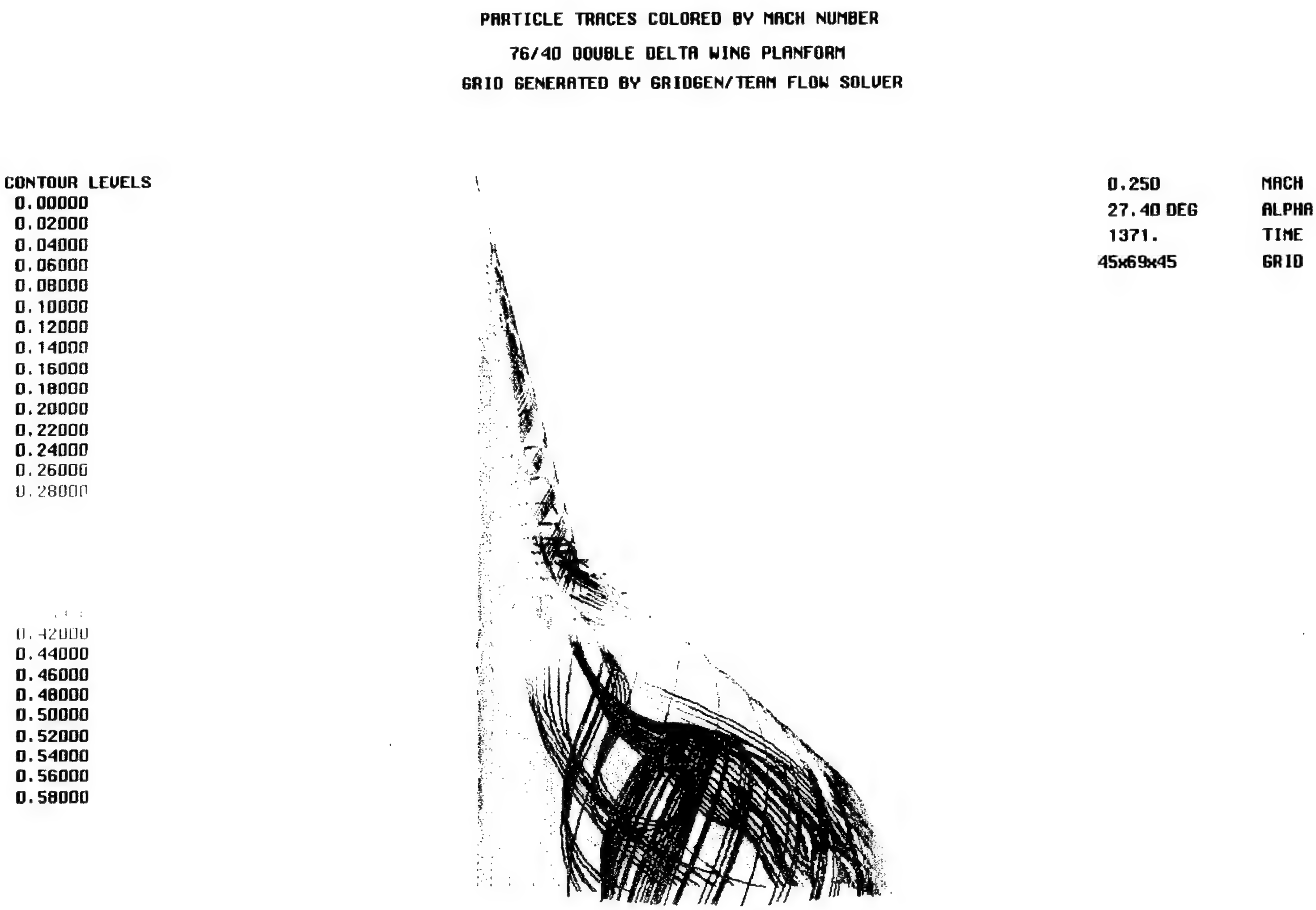

Figure 7. Detailed particle trace for α=27.4 degrees.

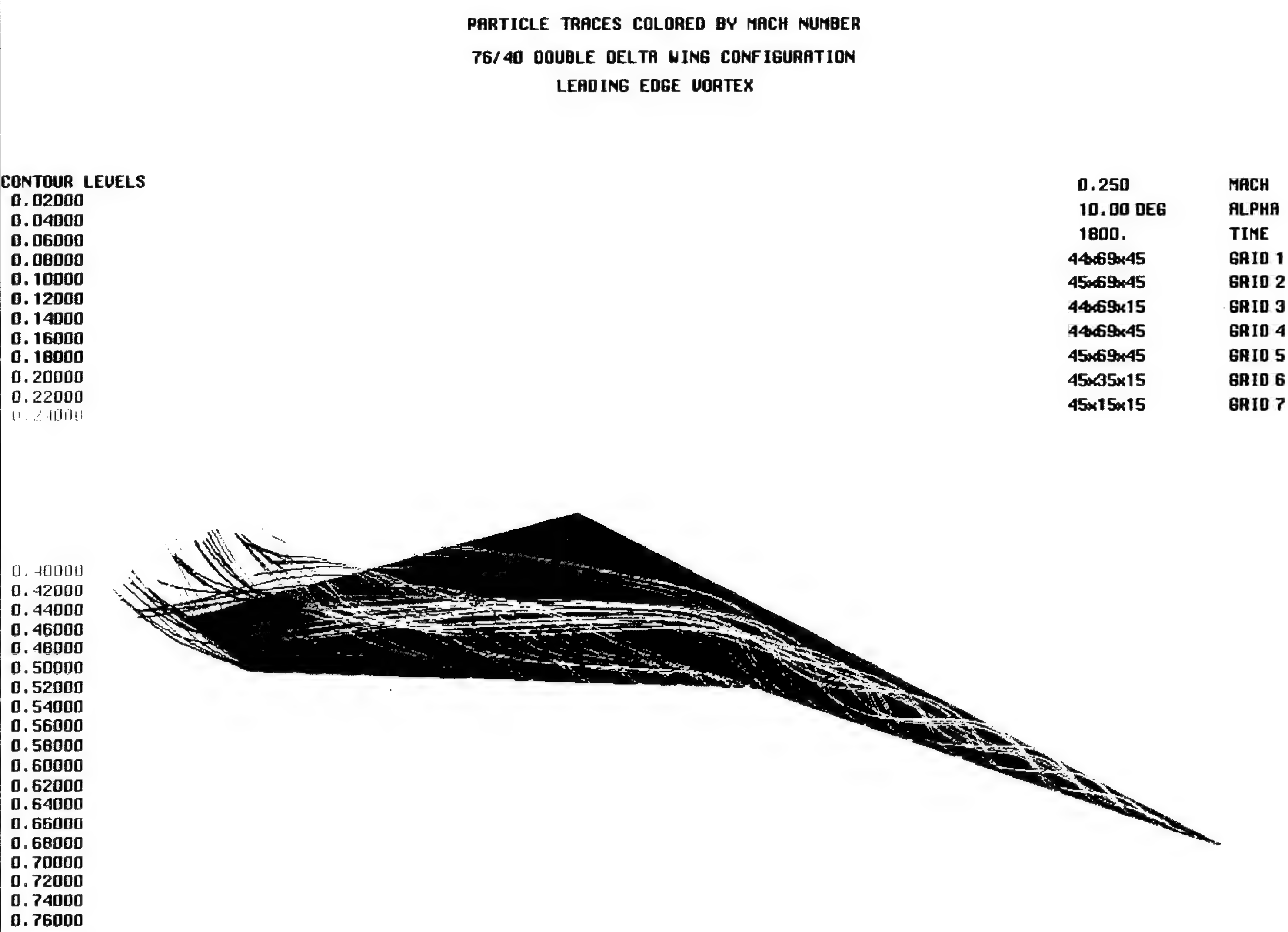

Figure 8. Leading edge vortex pattern, α=10.0 degrees.

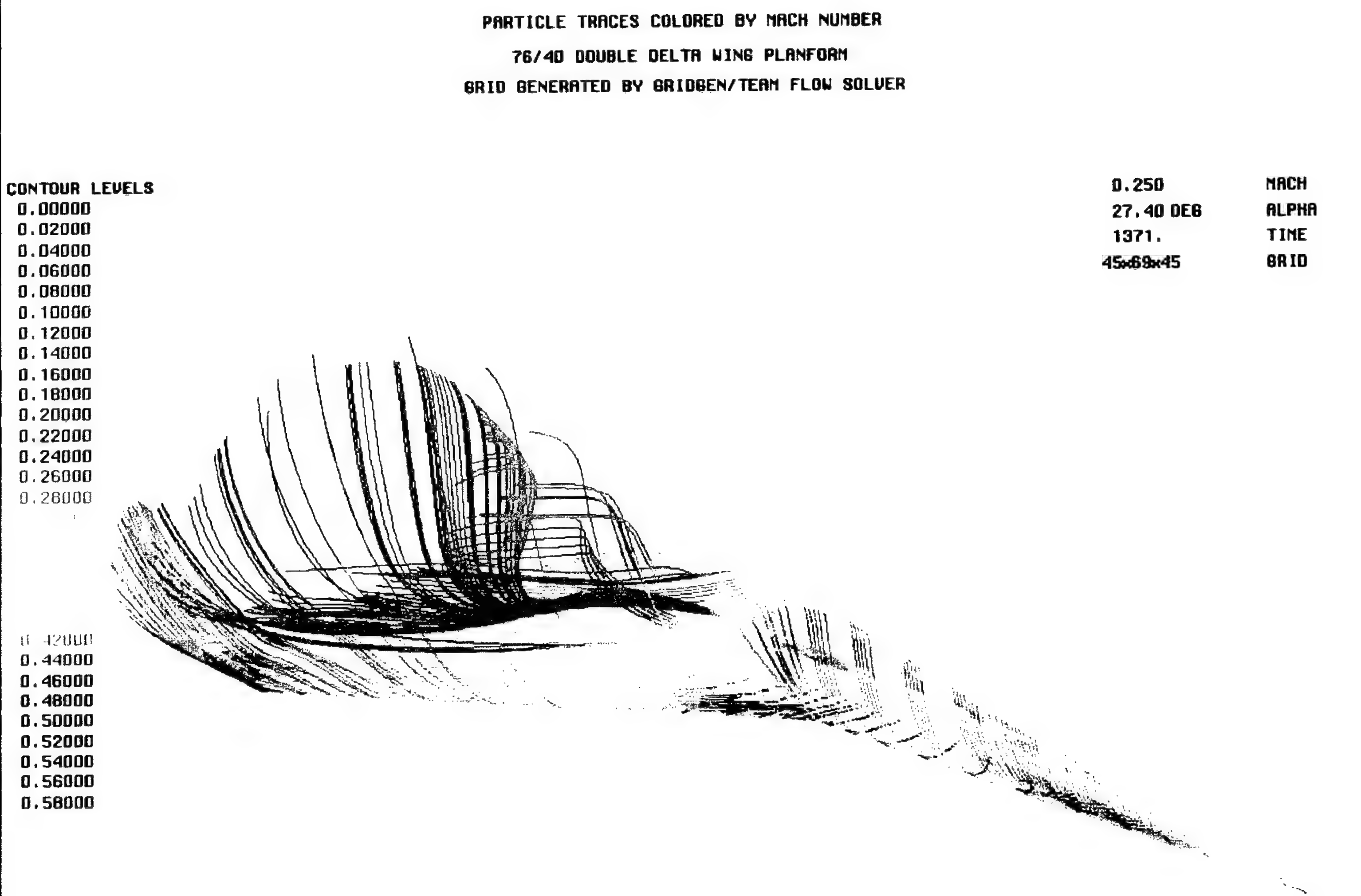

Figure 9. Leading edge vortex pattern, α=27.4 degrees.

Table 1. Slot Temperature Results

Baseline Model Peak Temp = 576 °F

w/h	Peak Temp °F	Source of Heating Data
	Cavity Windward Wall	
2.0	1,486	Figure 1 (Reference 1)
2.0	1,458	Figure 4 (Reference 1)
1.0	1,327	Figure 4 (Reference 1)
0.5	543	Figure 4 (Reference 1)
	Cavity Leeward Wall	
2.0	755	Figure 2 (Reference 1)
2.0	854	Figure 4 (Reference 1)
1.0	592	Figure 4 (Reference 1)
0.5	494	Figure 4 (Reference 1)

4.0 Summary

NASTRAN finite element models of an actively cooled leading edge were created to analyze joint/seal concepts. The heat exchanger designs analyzed utilized convection cooling employing cryogenic fluid flow in channels in the leading edge panels. Analysis was conducted using both CSA NASTRAN and MSC NASTRAN on Wright-Patterson computer systems. Thermal analyses, involving convection, conduction, and radiation, were run to obtain steady state temperature distributions in the finite element model.

A plain two-dimensional representation of a section across the channels of a simple lap joint between two cooling panels was used to analyze convection cooling in an Incoloy 909 design. An analysis was also performed on the model to assess the effects of radiation in providing additional cooling or heating on the surface and in the slot between two panels.

A 3-D model was created and used to investigate the 3-D effect where the heating flux on the leading edge changes rapidly with distance from the stagnation area on the leading edge tip, whereas the 2-D model implicitly assumed the flux to be constant along the length of the channels. The coolant coefficient and temperature of the coolant was also varied along the channels. Heat exchanger designs using AMZIRC, Incoloy 909, and NARloy-Z were created and analyzed.

A model with a variable width slot between the two adjacent edges was created and analyzed to investigate the effect of aerodynamic heating in the slot between two heat exchanger panels. This model was used to investigate heating in the slot as a function of the slot width and depth and determine the effect on the temperature distribution in the heat exchanger panels. The material simulated in this analysis was RSR 654. This analysis showed that the slot width needs to be controlled to less than 0.05 inches.

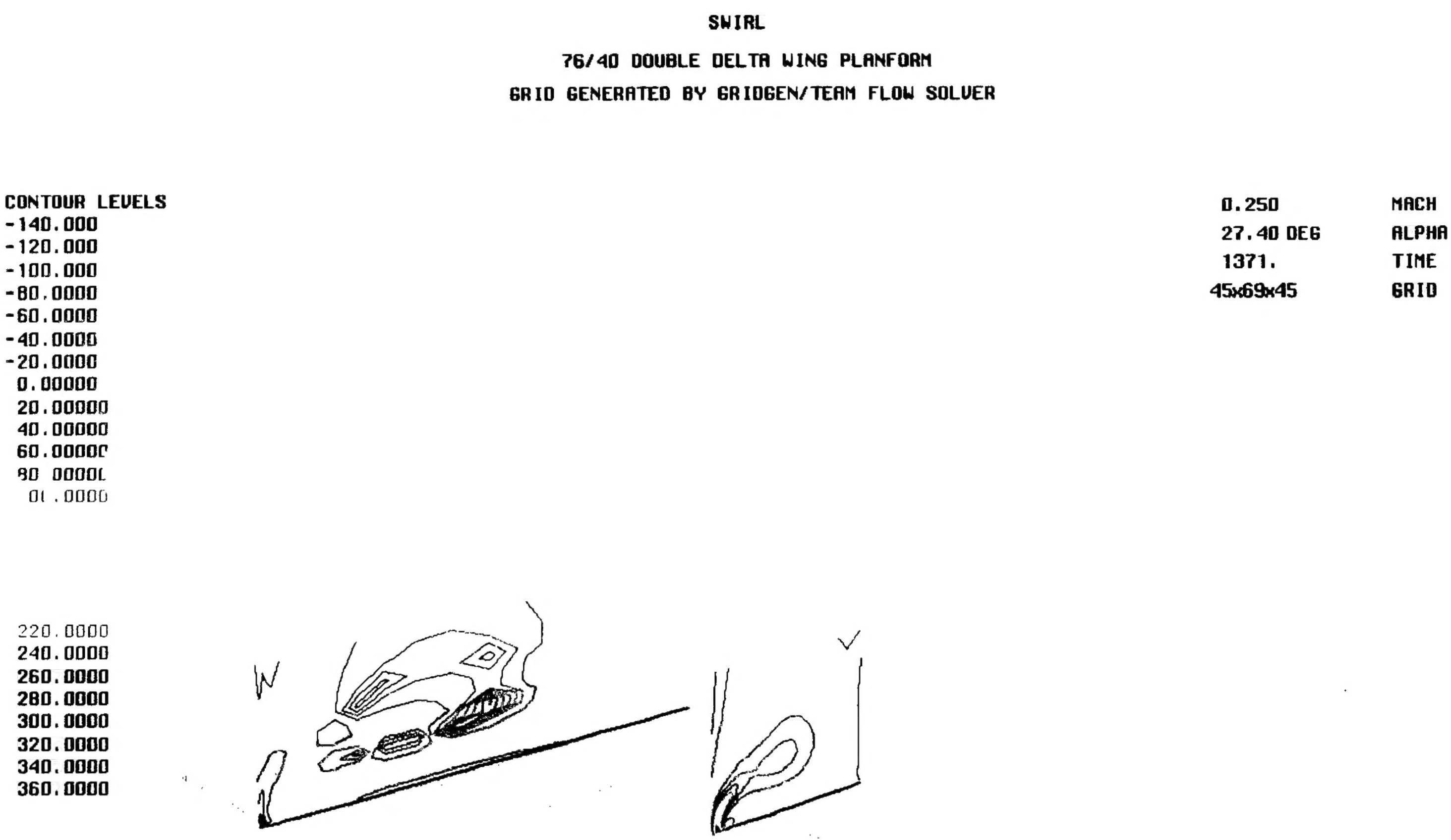

Figure 13. Swirl magnitude at .55c and .85c, α=27.4 degrees.

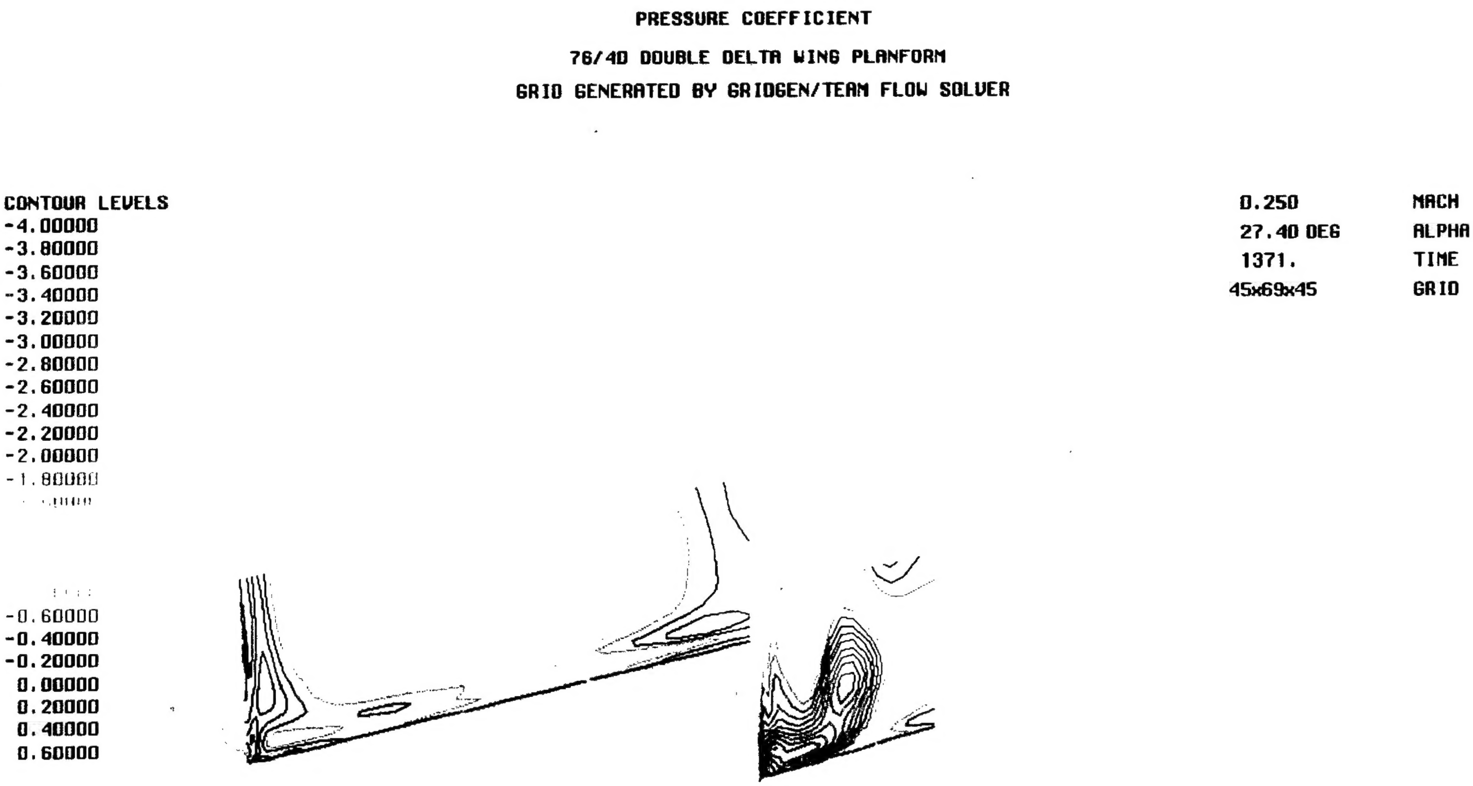

Figure 14. Pressure coefficient at .55c and .85c, α=27.4 degrees.